Contour Control for Ball Screw System with Asymmetric Friction

M2014SC024 Takayuki YAMAMOTO
Supervisor : Isao TAKAMI

Abstract

This paper proposes the method of the contour control. Tracking reference is achieved by the Perfect tracking control(PTC). Friction is compensated by the disturbance observer(DOB). By the experiments, the asymmetric of the friction is observed. In simulation and design of the DOB, the asymmetric of the friction is considered. The effectiveness of the proposed method is verified by the simulations and experiment.

1 Introduction

In servo system, point to point(PTP) control or contour control are required. PTP control is making the object move to the other point without considering the route. Contour control is making the object move along the predefined route. Many methods are proposed for the contour control of x-y ball screw system[1][2][3]. Perfect Tracking Control(PTC) is also used for the contour control[4]. PTC is a kind of the two degree-of-freedom and consists of the feedback controller and the feedforward controller. It achieves tracking control at each sampling time. If the model used in design of PTC is similar to the real system, the feedforward controller is effective and the contour control is achieved by the PTC. However, the real system is affected by the disturbance. In this study, ball screw system is used as the servo system. The ball screw system is widely used in positioning control. It is not easily affected by the friction. However, the effect of the friction is not negligible in the precise control. Even if the PTC is designed completely, tracking control may not be achieved due to the effect of the friction. Therefore, the friction must be compensated. Although many friction compensation methods are proposed, disturbance observer(DOB) is a kind of the effective methods[5][6].

In this study, PTC is adopted to achieve the contour control. PTC is designed based on [4]. However, since PTC is designed for the linear system, the performance of the PTC deteriorates for the system affected by the friction. If DOB compensates the disturbance, the behavior of the real system is similar with that of the linear system. Therefore, DOB based on LuGre model[5] is adopted to compensate the friction. To design the DOB, the parameters of the friction are identified. In identification, the asymmetric of the friction is observed. In other words, some parameters of the friction vary depending on the sign of the velocity. Therefore, design of the DOB and simulation are conducted based on the friction model, which depends on the sign of the velocity[6][7]. It is difficulty to implement this DOB because it is necessary to solve the Riccati equation at the each sampling time. In this study, the observer gain depending on the velocity is derived and it is approximated to the polynomial before implementing the controller. The polynomial depending on the velocity is implemented instead of the real observer gain. The effectiveness of the control system including the PTC and the DOB is verified by simulation and experiments.

The notation of A_{nm} stands for the elements of n rows m columns in A.

2 Modeling of The Ball Screw System

The overview of the ball screw system is shown in Figure 1. This system consists of the motors, the encoders, ball screw and table. The table is mounted on the ball screw. The table position is controlled by converting the rotational motion of the motor into linear motion through the ball screw. The motors are AC servo motors, which are controlled by the servo amplifiers. Thanks to the servo amplifiers, the arbitrary torques are given for the motors. The encoder measures the angle of the motor. The resolution of it is 2.5×10^5[plus/rev]. In this research, the lower ball screw system and the upper one are regarded as X axis and Y axis, respectively. Although it is necessary to obtain the model for each axis, the motion equation is the same as each other. Therefore, the model for X axis is derived. For X axis, let the angle of the motor, input torque for the motor and the state space vector be $\theta(t)$[rad], $T(t)$[Nm] and $x_m(t) = [\theta(t) \quad \dot{\theta}(t)]^T$. The state space representation is obtained as Eq. (1).

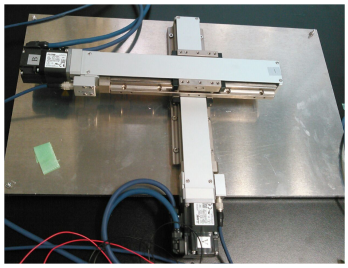

Figure 1 The picture of the ball screw system

$$\begin{aligned} \dot{x}_m(t) &= A_m x_m(t) + B_m u(t) \\ y(t) &= C_m x_m p(t) \end{aligned} \tag{1}$$

$$A_m = \begin{bmatrix} 0 & 1 \\ 0 & -\frac{R^2\sigma_0}{J+R^2M} \end{bmatrix}, B_m = \begin{bmatrix} 0 \\ \frac{1}{J+R^2M} \end{bmatrix},$$

$$C_m = \begin{bmatrix} 1 & 0 \end{bmatrix}$$

The physical parameters in Eq.(1) are shown in Table 1.

Table 1 Parameters of Ball Screw System

moment of inertia	J[Nms^2]	1.14×10^{-5}
mass of table	M[kg]	2.988
ball screw constant	R[m/rad]	$0.002/2\pi$

3 Modeling and Identification of The Friction

The schematic diagram of the LuGre model is represented in Figure 2. In Figure 2, there are many bristles on the contact surfaces between the two objects. Let the average displacement of the bristles and the velocity of

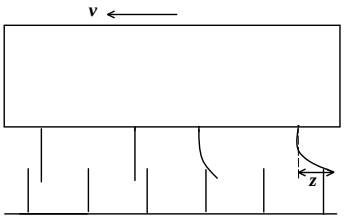

Figure 2 The schematic diagram of the LuGre model

the contact surface be z[m] and v[m/s]. The friction force F_L is represented by the following equations[7].

$$F_L = \sigma_0 z + \sigma_1 \dot{z} + \sigma_2 v \tag{2}$$

$$\dot{z} = v - \sigma_0 \frac{|v|}{g(v)} z \tag{3}$$

$$g(v) = (F_c + (F_s - F_c)e^{-|v/v_s|}) \tag{4}$$

The parameters for the LuGre model are shown in Table 2. To use the LuGre model in simulations and design

Table 2 Parameters of LuGre Model

spring constant of the bristle	σ_0[N/m]
viscous constant of the bristle	σ_1[Ns/m]
the viscous friction coefficient	σ_2[Ns/m]
static friction force	F_s[N]
Coulomb friction force	F_c[N]
Stribeck velocity	v_s[m/s]

of the controller, the parameters shown in Table 2 must be obtained. As the results of the identification, σ_0, σ_1 and σ_2 are identified as 2733×10^4[N/m], 95000[Ns/m] and 1083[Ns/m]. F_c, F_s and v_s are identified as 11[N], 15[N] and 1083[Ns/m]. However, the Coulomb friction force F_c and the static friction force F_s vary depending on the sign of the velocity[6][7]. In [6], friction models is described by Eq. (2), Eq. (3) and Eq. (5).

$$g(v) = \begin{cases} F_{c+} + (F_{s+} - F_{c+})e^{-|v/v_s|} & (v > 0) \\ F_{c-} + (F_{s-} - F_{c-})e^{-|v/v_s|} & (v < 0) \\ (F_{s+} + F_{s-})/2 & (v = 0) \end{cases} \tag{5}$$

In this study, the asymmetric of the friction is observed. In other words, $F_{c+} \neq F_{c-}$ and $F_{s+} \neq F_{s-}$. Therefore, let F_c and F_s be F_{c+} and F_{s+}. With using the same methods for F_{c+} and F_{s+}, F_{c-} and F_{s-} are identified as 25[N] and 27[N].

4 Deign of The Controller System

In this chapter, the controller system is designed. The controller system consists of PTC and disturbance observer based on LuGre model. Tracking control is achieved by the PTC. The structure of PTC is shown in Figure 3. As can be seen in Figure 3, the PTC consists of the feedforward controller $C_1[z]$ and the feedback controller $C_2[z]$. First, the feedback controller $C_2[z]$ is designed to constitute the PTC. In this study, the feedback controller $C_2[z]$ is LQ controller. Next, the feedforward controller $C_1[z]$ is designed. However, the PTC is designed for the linear system which does not include the friction F_L. Therefore, the disturbance observer based on LuGre model is used to compensate the friction.

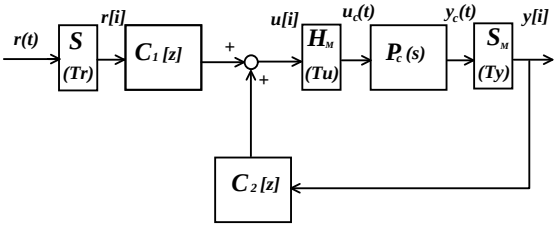

Figure 3 The structure of the PTC

First, discrete LQ controller is designed for Eq. (1). To obtain discrete-time system, let the new state vector be $x_{md}(k) = [\theta_d(k)\ \dot{\theta}_d(k)]^T$. Eq. (1) is transformed into Eq. (6).

$$x_{md}(k+1) = A_{md}x_{md}(k) + B_{md}u(k) \tag{6}$$

Here, $A_{md} = \mathrm{e}^{A_m T_s}$, $B_{md} = \int_0^{T_s} \mathrm{e}^{A_m \tau} B_m d\tau$. T_s is sampling time and k is the time index that indicates kth sampling time. For Eq. (6), the controller is designed to minimize the following cost function.

$$J_{ev} = \sum_{i=0}^{\infty} [x_{md}(k)^T Q_{cd} x_{md}(k) + u(k)^T R_{cd} u(k)] \tag{7}$$

Q_{cd} is the weight matrix for the state and R_{cd} is the weight matrix for the control input. If there exists $P > 0$ satisfying Eq. (8), the controller $u(k) = Fx_{md}(k) = -(R_{cd} + B_{md}^T P B_{md})^{-1} B_{md}^T A_{md} x_{md}(k)$ is obtained.

$$\begin{aligned} &A_{md}^T P A_{md} + Q_{cd} - P - A_{md}^T P B_{md} \\ &(R_{cd} + B_{md}^T P B_{md})^{-1} B_{md}^T P A_{md} = 0 \end{aligned} \tag{8}$$

Next, $C_1[z]$ is designed to track reference. As can been seen in Figure 3, there are two sampler S, S_M and a holder H_M for reference $r(t)$, output $y(t)$ and control input $u(t)$. Let the each sampling period be T_r, T_y and T_u, respectively. In this study, $T_y = T_u$ and T_r is nT_u. Here, n is the order of $P_c(s)$. Let the longest sampling period T_r be the flame sampling period T_f. To design the the multirate sampling controller $C_1[z]$, the method proposed in [4] is used. Let the state vector be $x[i] = x_m(iT_f)$. The discrete-time system at the sampling period T_f is obtained by the following equation.

$$x[i+1] = Ax[i] + Bu[i], y[i] = Cx[i] + Du[i] \tag{9}$$

The multirate feedforward controller $C_1[z]$ is obtained by the following equation[4].

$$C_1[z] = (M - C_2 N)K \tag{10}$$

$$M = \left[\begin{array}{c|c} A+BF & B \\ \hline F & I \end{array}\right] = I + z^{-1}FB,$$

$$N = \left[\begin{array}{c|c} A+BF & B \\ \hline C+DF & D \end{array}\right] = D + z^{-1}(C+DF)B,$$

$$F = -B^{-1}A, K = B^{-1}$$

Finally, the disturbance observer proposed in [5] is adopted to compensate the friction. This disturbance observer is discrete time system. To design it, Eq. (3),

the state equation about the bristle, is discretized. Eq. (11) is obtained.

$$z_d(k+1) = \mathrm{e}^{(-\sigma_0\alpha(\dot{\theta}_d(k))T_s} z_d(k) - \frac{\mathrm{e}^{(-\sigma_0\alpha(\dot{\theta}_d(k)))T_s} - 1}{\sigma_0\alpha(\dot{\theta}_d(k))} R\dot{\theta}_d(k) \quad (11)$$

$$\alpha(\dot{\theta}(k)) = \frac{|R\dot{\theta}(k)|}{g(R\dot{\theta}_d(k))} \quad (12)$$

Let the estimated vector be $\hat{x}_{Ld}(k) = [\hat{\theta}_d(k) \ \hat{\dot{\theta}}_d(k) \ \hat{z}(k)]^T$. From Eq. (2), Eq. (6) and Eq. (11), the disturbance observer is obtained by the following equation.

$$\hat{x}_{Ld}(k+1) = A_{Ld}(\hat{\dot{\theta}}_d(k))x_{Ld}(k) + B_{Ld}u_d(k) + K_{Ld}(\hat{\dot{\theta}}_d(k))(\theta_d(k) - \hat{\theta}_d(k)) \quad (13)$$

$$\hat{y}_{Ld} = C_{Ld}\hat{x}_{Ld}(k) \quad (14)$$

$$A_{Ld11}(\hat{\dot{\theta}}_d(k)) = A_{md} + \begin{bmatrix} O & -B_{mgd1}\sigma_0 \end{bmatrix},$$
$$A_{Ld12}(\hat{\dot{\theta}}_d(k)) = -B_{mgd2}(\sigma_0 - \sigma_0\sigma_1\alpha(v_d(k))),$$
$$A_{Ld21}(\hat{\dot{\theta}}_d(k)) = O + \begin{bmatrix} O & -a_f \end{bmatrix}, A_{Ld22}(\hat{\dot{\theta}}_d(k)) = b_f,$$
$$B_{mgd1} = \int_0^{Ts} e^{A_m\tau}B_{mg1}d\tau, B_{mg1} = \begin{bmatrix} 0 \\ R/(J+R^2) \end{bmatrix},$$
$$B_{mgd2} = \int_0^{Ts} e^{A_m\tau}B_{mg2}d\tau, B_{mg2} = \begin{bmatrix} 0 \\ R^2/(J+R^2) \end{bmatrix},$$
$$B_{Ld} = \begin{bmatrix} B_{md} \\ O \end{bmatrix}, a_f = \frac{\mathrm{e}^{(-\sigma_0\alpha(\dot{\theta}_d(k)))T_s} - 1}{\sigma_0\alpha(\dot{\theta}_d(k))}R,$$
$$b_f = \mathrm{e}^{(-\sigma_0\alpha(\dot{\theta}_d(k))T_s}, C_{Ld} = \begin{bmatrix} 1 & 0 & 0 \end{bmatrix}$$

Here, $K_{Ld}(\hat{\dot{\theta}}_d(k))$ is observer gain. The estimated friction force is obtained by the following equation.

$$\hat{F_L} = \begin{bmatrix} O & \sigma_1 & \sigma_0 - \sigma_0\sigma_1\alpha(\hat{\dot{\theta}}_d(k)) \end{bmatrix} \hat{x}_{Ld(k)}$$

From [5], the observer gain is defined by Eq. (15).

$$K_{Ld}(\hat{\dot{\theta}}_d(k)) = A_{Ld}(\hat{\dot{\theta}}_d(k))P_{Ld}(\hat{\dot{\theta}}_d(k))C_{Ld}^T \{(R_{cd} + C_{Ld}P_{Ld}(\hat{\dot{\theta}}_d(k))C_{Ld}^T)^{-1}\}^T \quad (15)$$

$P_{Ld}(\hat{\dot{\theta}}_d(k)) > 0$ is satisfying with Eq. (16).

$$A_{Ld}(\hat{\dot{\theta}}_d(k))P_{Ld}(\hat{\dot{\theta}}_d(k))A_{Ld}(\hat{\dot{\theta}}_d(k))^T + Q_{Ld} - P_{Ld}(\hat{\dot{\theta}}_d(k)) - A_{Ld}(\hat{\dot{\theta}}_d(k))PC_{Ld}^T(R_{Ld} + C_{Ld}P_{Ld}(\hat{\dot{\theta}}_d(k))C_{Ld}^T)^{-1}C_{Ld}PA_{Ld}(\hat{\dot{\theta}}_d(k))^T = 0 \quad (16)$$

In Eq. (15) and Eq. (16), R_{Ld} and Q_{Ld} are the weight matrix for the estimated state and the weight matrix for the observed output, respectively. Eq.(16) varies at each sampling time. The observer gain $K_{Ld}(\hat{\dot{\theta}}_d(k))$ is obtained by finding $P_{Ld}(\hat{\dot{\theta}}_d(k))$ satisfying with Eq. (16) at each sampling time.

5 Simulations and Experiments

The conditions for the controller are described. The sampling times T_y, T_u and T_s are 0.001[s]. The sampling times T_r is 0.002[s]. The weight matrices in LQ controller and the weight matrices in DOB are defined as follows.

$$Q_{cd} = diag\begin{bmatrix} 10 & 1 \end{bmatrix}, R_{cd} = 1$$
$$Q_{Ld} = diag\begin{bmatrix} 1 & 1 & 1 \end{bmatrix}, R_{Ld} = 10^9$$

The following two controller are implemented in simulations and experiments.

- Symmetric controller: This controller does not depend on the sing of velocity. In other words, it uses the DOB designed for Eq.(4).
- Asymmetric controller: This controller depend on the sing of velocity. In other words, it uses the DOB designed for Eq.(5).

In section 4, The observer gain $K_{Ld}(\hat{\dot{\theta}}_d(k))$ is obtained by finding $P_{Ld}(\hat{\dot{\theta}}_d(k))$ satisfying with Eq. (16) at each sampling time. Therefore, it is difficulty to implement this disturbance observer. To avoid this difficulty, the observer gain $K_{Ld}(\hat{\dot{\theta}}_d(k))$ is approximated to polynomial in velocity domain. In this study, the full speed is not so high because the reference of the precise control is very small. The velocity range is defined as between 2 [rad/s] and −2 [rad/s]. As a example, the observer gain is approximated at the positive velocity region. The observer gain $K_{Ld}(\hat{\dot{\theta}}_d(k))$ is shown in Figure 4. Let the

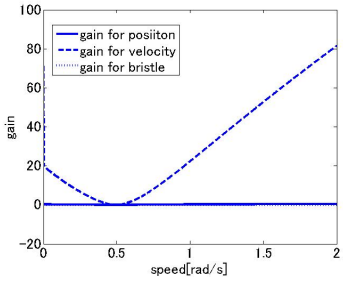

Figure 4 The observer gain in the plus velocity domain

elements of the $K_{Ld}(\hat{\dot{\theta}}_d(k))$ be the following equation.

$$K_{Ld}(\hat{\dot{\theta}}_d(k)) = \begin{bmatrix} K_{Ld1}(\hat{\dot{\theta}}_d(k)) & K_{Ld2}(\hat{\dot{\theta}}_d(k)) & K_{Ld3}(\hat{\dot{\theta}}_d(k)) \end{bmatrix}^T$$

In Fig. 4, the gain for position, the gain for speed and the gain for bristle represent $K_{Ld1}(\hat{\dot{\theta}}_d(k))$, $K_{Ld2}(\hat{\dot{\theta}}_d(k))$ and $K_{Ld3}(\hat{\dot{\theta}}_d(k))$, respectively. To implement the disturbance observer, $K_{Ld}(\hat{\dot{\theta}}_d(k))$ is approximated to fourth degree polynomial. The result of it is shown in in Figure 5. In Figure 5, the solid line, the dashed line and the

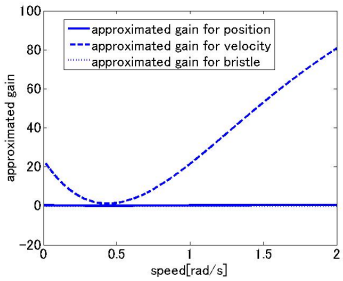

Figure 5 The observer gain in the plus velocity domain

dotted line approximate $K_{Ld1}(\hat{\dot{\theta}}_d(k))$, $K_{Ld2}(\hat{\dot{\theta}}_d(k))$ and $K_{Ld3}(\hat{\dot{\theta}}_d(k))$, respectively. As can be seen in Figure 4 and Figure 5, the approximated gain represents the observer gain sufficiently. Using the same way, the gain is approximated at the negative velocity region.

In simulation, Eq.(5) is used. Two simulations are conducted. In first one, the reference is $r(t) = \frac{\pi}{10}sin(\frac{\pi}{15})t$ [rad]. In second one, the reference is $r(t) = \frac{\pi}{100}sin(\frac{\pi}{15})t$

[rad]. The first simulation results are shown in Figure 6. Figure 6 shows the motor angle. As can be seen

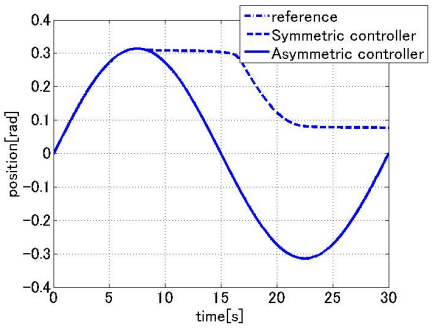

Figure 6 The first simulation of output when the reference is $r(t) = \frac{\pi}{10} sin(\frac{\pi}{15})t$ [rad].

in Figure 6, the symmetric controller does not achieve tracking reference. The asymmetric controller achieves tracking reference. The second simulation results are shown in Figure 7. Figure 7 shows the motor angle.

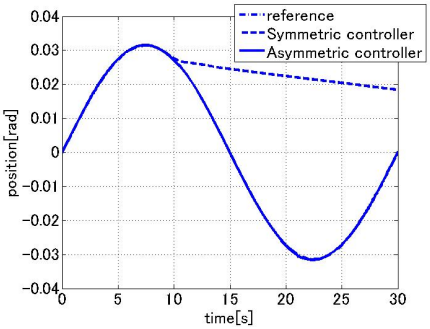

Figure 7 The first simulation of output when the reference is $r(t) = \frac{\pi}{100} sin(\frac{\pi}{15})t$ [rad].

As can be seen in Figure 7, the symmetric controller does not achieve tracking reference. The asymmetric controller achieves tracking reference.

Next, Two experiments are conducted. In first one, the reference is $r(t) = \frac{\pi}{10} sin(\frac{\pi}{15})t$ [rad]. In second one, the reference is $r(t) = \frac{\pi}{100} sin(\frac{\pi}{15})t$ [rad]. The first experiment results are shown in Figure 8. Figure. 8 shows the motor angle. As can be seen in Figure 8, the symmetric controller does not achieve tracking reference. The asymmetric controller achieves tracking reference. The second experiment results are shown in Figure 9. Figure 9 shows the motor angle. As can be seen in Figure 9, the symmetric controller does not achieve tracking reference. The asymmetric controller achieves tracking reference.

6 Conclusion

In this study, the method for the precise contour control is proposed. The PTC is designed to track reference. The disturbance observer is designed to compensate the friction. Moreover, the asymmetric of the friction is considered in simulation and design of the DOB. The effectiveness of the proposed control system is verified by the simulations and the experiments.

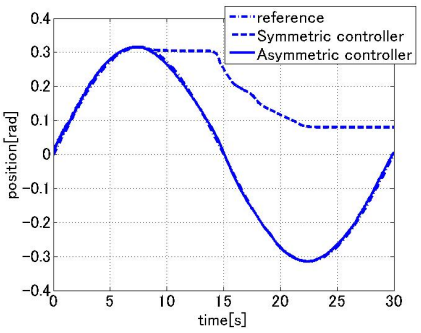

Figure 8 The first experiment of output when the reference is $r(t) = \frac{\pi}{10} sin(\frac{\pi}{15})t$ [rad].

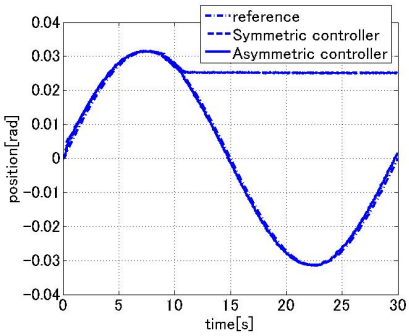

Figure 9 The first experiment of output when the reference is $r(t) = \frac{\pi}{100} sin(\frac{\pi}{15})t$ [rad].

References

[1] M. J. Patrick, N. Ishak and R. Adnan: "Contouring control of non-minimum phase xy table system using trajectory ZPETC," International journal of scientific and technology research, Vol. 1, No. 6, pp.80-85, 2012

[2] Li. HongSheng, Z. Xingpeng and C. Y. Quan: "Iterative learning control for cross-coupled contour motion system," IEEE International Conference on Mechatronics and Automation, Vol. 3, pp.1468-1472, 2005

[3] H. Chuxiong, Y. Bin and W. Qingfeng: "Coordinated adaptive robust contouring controller deign for an industrial biaxial precision gantry," IEEE ASME Transactions on Mechatronics, Vol. 15, No. 5, pp.728-735, 2010

[4] H. Fujimoto, Y. Hori and A. Kawamura: "Perfect tracking control method based on multirate feedforward control," Transactions of the Japan Society of Mechanical Engineers, Series C, Vol. 59, No.565, pp.2707-2711 1993

[5] D. Hoshino and J. Ishikawa: "Friction compensation using time variant disturbance observer based on the LuGre model," Transactions of the Japan Society of Mechanical Engineers, Series C, Vol. 79, No.805, pp.3206-3220, 2013

[6] L. Freidovich, A. Rbertsson, A. Shiriaev and R. Johansson: "LuGre-Model-Based friction compensation," IEEE Transactions on Control Systems Technology, Vol. 18, No. 1, pp.194-200, 2010

[7] K. J. Astrom and C. D. Canudas: "Revisiting the LuGre friction model," IEEE Control Systems, Vol. 28, No. 6, pp.101-114, 2008